International Journal of Fatigue 134 (2020) 105507

Contents lists available at ScienceDirect

International Journal of Fatigue

journal homepage: www.elsevier.com/locate/ijfatigue

A continuum fatigue damage model for the cyclic thermal shocked ceramic-matrix composites

Zhengmao Yang[a,*], Hui Liu[b]

[a] Institute of Mechanics, Chinese Academy of Sciences, Beijing, China
[b] School of Aerospace Engineering, Tsinghua University, Beijing, China

ARTICLE INFO

Keywords:
Ceramic-matrix composites (CMCs)
Fatigue modeling
Damage accumulation
Plastic deformation

ABSTRACT

In the present work, the tension-compression fatigue behavior of the 2-D woven oxide/oxide-ceramic-matrix composites is investigated. Experimental investigations reveal different fatigue failure mechanism for the original and the cyclic thermal shocked ox/ox-CMCs, and both materials undergo cyclic softening in the whole loading history. Based on the decrease of the elastic modulus, a new fatigue damage model is proposed to characterize the fatigue damage evolution and predict the fatigue life of both the original and the cyclic thermal shocked ox/ox-CMCs. The total damage is separated into the thermal stress-related damage from thermal shocks and the fatigue damage from applied mechanical loads. The good agreement between the proposed model and experimental data indicates that the damage model has the potential to describe complex thermomechanical damage of the ox/ox-CMCs under coupled cyclic thermal shocks and mechanical loading.

1. Introduction

Oxide/oxide-ceramic-matrix composites (ox/ox-CMCs), capable of outstanding long-term mechanical properties in severe temperature and oxidizing environments, are excellent candidate materials for advanced applications such as aerospace propulsion components and thermal protection systems for re-entry vehicles [1–4]. More essentially, the thermal shock resistance and fatigue resistance of ox/ox-CMCs are vital issues, as they may fail under transient thermal conditions due to their low thermal conductivity and low fracture toughness. Therefore, there is considerable interest in the investigation of cyclic thermal coupling mechanical fatigue loading for ox/ox-CMCs, in order to understand their fatigue behavior in the transient thermal environments.

Thermal shock-induced damage mechanisms and damage accumulation in fiber-reinforced CMCs have been the subject of many investigations [5,6]. Unfortunately, due to the highly transient processes of damage and the restrictions of the temporal and spatial resolution for the current experimental methods, it is difficult to do the in-situ observations during thermal shocks. Thus, the understanding of the mechanical performance evolution during coupling cyclic thermal shock with mechanical fatigue loading is still limited. Yang et al. [7–9] investigated cyclic thermal shock-induced thermomechanical damage in the ox/ox-CMCs, they found that microcracks in the matrix lead to the macroscopic damage, which is induced by the thermal stress during the shocks, and the elastic modulus degradation are driven by the energy density release rate [10]. However, although cyclic thermal shock is an essential kind of thermomechanical fatigue, the thermomechanical fatigue life of the composites cannot be effectively evaluated only by the cyclic thermal shocks.

Fatigue damage model of CMCs has been widely studied in the literature [11–13]. So far, two kinds of fatigue models have been introduced [14,15]: (i) Phenomenological models, including fatigue life models, residual strength model and residual stiffness model, and the fatigue damage mechanisms in composites are neglect; and (ii) Progressive damage models, indicated by damage variables related to measurable damage (delamination size, matrix cracks, etc.) [16], using fracture mechanics, damage mechanics and statistical approaches.

As for the phenomenological models, Lemaitre and Desmorat [10] developed a CDM fatigue damage model to analyze the fatigue damage evolution and predict the low cycle fatigue life. Chaboche et al. [17,18] established a nonlinear cumulative fatigue damage model using stress to predict the fatigue life under uniaxial loading, then discussed the influence of load sequence and average stress on the damage process. However, these models are specific to a particular composite, and do not consider meso-composition and damage mechanisms.

It is well-understood in the literature that progressive damage models can reflect the fatigue damage process of composite structures quantitatively. Min et al. [19] developed a micro-mechanics model

* Corresponding author.
E-mail address: zmyang@imech.ac.cn (Z. Yang).

https://doi.org/10.1016/j.ijfatigue.2020.105507
Received 15 September 2019; Received in revised form 18 January 2020; Accepted 21 January 2020
Available online 28 January 2020
0142-1123/

Nomenclature

b	the fatigue strength exponent
D	the damage variable
D_e	the elastic damage
D_f	the fatigue damage
D^{init}	the initial (pre-) damage contained in the material
D^{cr}	the critical damage variable in the material
E_0	the initial elastic modulus
E	the residual elastic modulus
σ_f'	the fatigue strength coefficient
K	the strength coefficient
K'	the cyclic strength coefficient
n	the strain hardening exponent
n'	the cyclic strain hardening exponent
N	the number of thermal shock cycles
S_f	the material parameter
T_{shock}	the thermal shock temperature
U	the strain energy
Y	the energy release rates
w	the model parameter
α	the damage exponent
η	the stress triaxiality
ε_a^p	the plastic strain amplitude
$\varepsilon_N^{unloading}$	the unloading composites strain for the N cycle
$\varepsilon_{N+1}^{reloading}$	the reloading composites strain the $N+1$ cycle
σ_a	the stress amplitude
$\widetilde{\sigma}_{eq}$	the effective stress
σ_{eq}^{max}	the maximum equivalent Mises stress in the whole loading history
σ_f	the fracture stress of in the monotonic tensile experiment
ν	the Poisson's ratio
$\bar{\omega}$	the effect of different strain energy components
ρ	the material density
$\bar{\omega}$	the model parameter
Υ	the hysteresis energy density
ΔW^p	the plastic strain energy density

combining the three-phase micro-mechanics, the continuum fracture mechanics and the shear-lag, to analyze the damage mechanism and fatigue failure and predict the fatigue life of the CMCs. Sabelkin et al. [20] investigated and characterized the influence of various parameters (loading type, loading level and environment) to the damage and failure mechanisms in SiC/SiC CMCs by simulated combustion environment. Benkabouche [21] predicted the fatigue damage evolution and the lifetime for the composites under different amplitudes and multiaxial cyclic loadings by proposing a modified nonlinear fatigue damage model. Li et al. [22] studied the effects of cyclic temperature range, fiber/matrix interface debonded energy, matrix cracking space and fiber volume fraction on the fatigue hysteresis loops of the long-fiber-reinforced CMCs under out-of-phase thermomechanical fatigue loadings. Rafiee et al. [23] applied the progressive damage modeling techniques in fiber reinforced-polymer composite lifetime prediction based on stiffness degradation, and performed the stochastic fatigue/static analysis in FRP pipes subjected to internal cyclic hydrostatic pressure, taking into account winding angle, fiber volume fraction, and mechanical properties as random parameters [24–26]. Although fatigue behavior of CMCs has been intensively studied, an essential research thrust is needed to achieve reliable fatigue damage modeling of the processes that take place under thermomechanical loading.

The principal objective of the present work is to develop a fatigue damage model to quantitatively describe uniaxial fatigue damage in both the original ox/ox-CMCs and cyclic thermal shocked ox/ox-CMCs properly. Toward this aim, firstly, fatigue tests under tension-compression loading are conducted to provide a database for identifying the fatigue damage evolution. Then, the cyclic stress-strain response, the residual stiffness evolution and fatigue failure mechanisms for the original ox/ox-CMCs and cyclic thermal shocked ox/ox-CMCs were also subjected to comparative analysis and discussed. Finally, an inelastic fatigue damage model is developed in the framework of continuum damage mechanics, coupling the Ramberg-Osgood cyclic plasticity model, to describe the evolution of fatigue damage under cyclic thermal shock coupling fatigue loading condition.

2. Material and experimental procedures

2.1. Materials

The test materials in the present work consisted of 2-D woven Nextel™ 610 fibers (99%α-Al_2O_3) and $Al_2O_3 - SiO_2 - ZrO_2$ matrix. Firstly, the uncoated Nextel™ 610 fibers were woven in eight harness satin weave (8HSW) and impregnated with the paste-like Al_2O_3 slurry using knife blade coating. Then 8 layers of woven fibers in the order of 0°/90° were stacked together, pressed and dried at 80 °C–150 °C, and sintered at 1100 °C–1300 °C, then infiltrated with 3YSZ-sol to perform the second sintering process for 5 h at the same temperature [27]. The matrix has a chemical constitution of 85% Al_2O_3 and 15% 3YSZ (in weight). The density of the original ox/ox-CMCs was approximately 2.71 g/cm^3, with the porosity of 27.6%, and the fiber volume fraction was about 44%. The uniaxial tension-compression fatigue specimens were cut into a shape of 160 mm × 20 mm by water jet (Fig. 1).

Fig. 2 shows the overall microstructure of the original ox/ox-CMCs. It illustrates some residual pores and extensive micro-cracking appear in the matrix. The voids arise during the material processing, which have been created by gas trapped with the matrix infiltrated fiber preform. Micro-cracking existed may due to different coefficients of

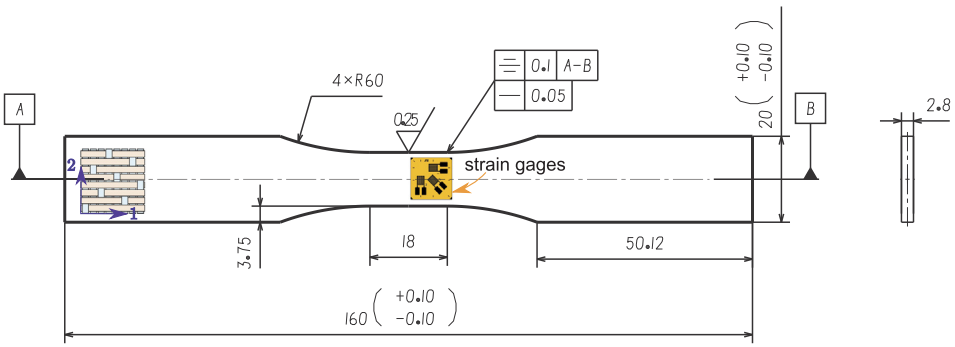

Fig. 1. Uniaxial tension-compression fatigue specimen geometry of the ox/ox-CMCs. All dimensions in mm.

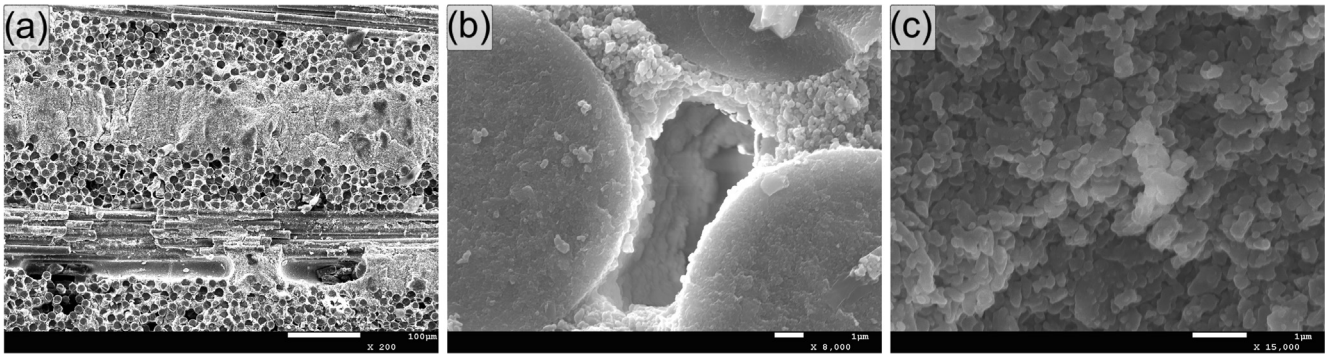

Fig. 2. The original 2-D woven ox/ox-CMCs: (a) overview, (b) fiber and matrix, (c) the porous matrix is evident.

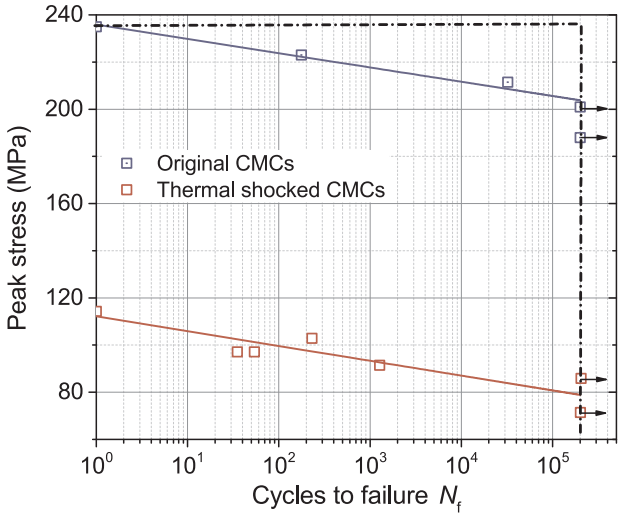

Fig. 3. Tension-compression fatigue $S-N$ curves for the original and cyclic thermal shocked ox/ox-CMCs in air (room temperature). Arrow indicates that failure of specimen did not occur when the test was terminated.

thermal expansion (CTE) for fiber and matrix causing excessive shrinkage during the material fabrication. These inherent defects play a significant role in mechanical properties, more general description of the effect of inherent defects will be discussed in a separate paper.

2.2. Thermal shock tests

Thermal shock tests were carried out by heating the specimens to a pre-determined temperature, then holding for 10 min to allow for temperature equilibrium, then drop the heated specimen into distilled water with room temperature. Opila [28] has confirmed that the mechanical properties of ox/ox-CMCs are very sensitive to water vapor at elevated temperatures. Therefore, after each water quenching, it is necessary to dry in air at room temperature before performing the next water quenching experiment. The maximum test temperature was set to 1100 ˚C, as these materials application is limited to 1200 ˚C. More manipulate details for the thermal shock tests can refer to [7,8].

It should be noted that after subjected to the cumulative 8 cycles of thermal shock (T_{shock} = 1100 °C), the cyclic thermal shock-induced thermomechanical damage is nearly saturated according to the prior work [8]. Consequently, the ox/ox-CMCs subjected to 8 cycles of thermal shock were selected in the present work to determine the fatigue performance of the composites after thermal shocks.

2.3. Tension-compression fatigue tests

Much research has been devoted to the tension-tension fatigue behavior of ox/ox-CMCs [29,30]. However, as the effect of compression on material behavior in service environments can not be neglect, it is critical to understand the tension-compression fatigue performance of ox/ox-CMCs.

Tension-compression fatigue tests were proceeded on a servo-controlled MTS mechanical testing machine under a constant amplitude

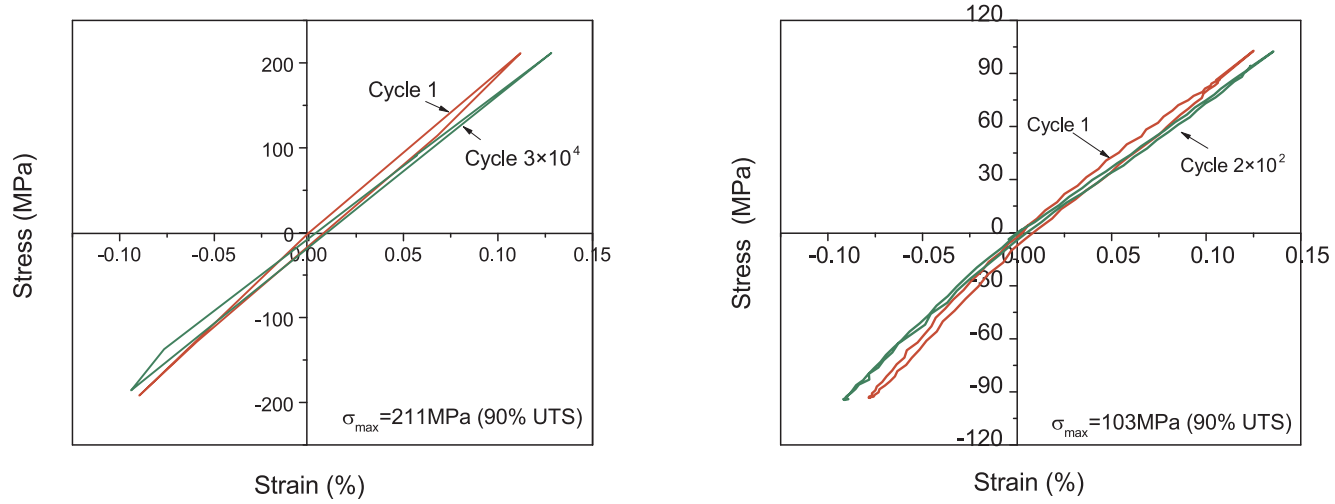

(a) The original ox/ox-CMCs (b) The cyclic thermal shocked ox/ox-CMCs

Fig. 4. Typical evolution of stress-strain hysteresis response of composites with fatigue cycles.

load controlled method. The fatigue test frequency was 1.0 Hz with the sinusoidal waveform, and the stress ratio was $R = -1$. All fatigue tests were conducted at room temperature. The fatigue stress level (σ_{max}), applied as a percentage of the ultimate tensile strength (UTS) obtained from the static tensile experiments, started from 62.5% to 90% average UTS. The max load cycle 2×10^5 was defined as the fatigue run-out, which was expected in aerospace applications. If the specimens survived over 2×10^5 cycles, the fatigue experiments would be interrupted. The MTS alignment fixture was used to precisely align the mechanical testing system before tests. The misalignment was limited to 0.015% of bending for tension-compression fatigue specimens to prevent buckling failure in all tests.

The cyclic stress-strain data were recorded for each test, so that variations in maximum and minimum strains, as well as elastic modulus change in fiber-reinforced direction (direction 1) in the process, could be examined. After tension-compression fatigue tests, the scanning electron microscope (SEM) was used to examine the fracture surfaces of specimens.

3. Experimental results and discussion

3.1. $S - N$ curve

Fig. 3 shows the maximum stress vs. cycles to failure ($S - N$) curves for the original and cyclic thermal shocked ox/ox-CMCs (the data with arrows (the run-out data) represents the interrupted experiments).

It is noteworthy that all fatigue failures occur in the compressive stage of the fatigue cycle. The room-temperature fatigue limit achieves 85% UTS for the original ox/ox-CMCs, which is similar to other CMCs exhibiting fatigue limits of 80%-95% UTS. However, the fatigue behavior for the cyclic thermal shocked ox/ox-CMCs is unlike that observed for the original materials. The fatigue run-out stress level of the cyclic thermal shocked ox/ox-CMCs is only 75% UTS, which is closely associated with matrix-cracks and delamination exhibiting. There is crack opening and closing, interphase friction between the fiber and matrix in the composites, resulting in the loss in ultimate fatigue strength of about 10%. It indicates that the fatigue performance of ox/ox-CMCs is significantly degraded in the presence of cyclic thermal shock processing.

The fatigue life degradation in ox/ox-CMCs is observed to depend on the applied stress, frequency, stress ratio and test environments [29]. Evolution of hysteresis stress-strain response with cycles of the original and cyclic thermal shocked ox/ox-CMCs is typified in Fig. 4. It should be noted that the hysteresis response of the cyclic thermal shocked ox/ox-CMCs is quite similar to that for the original materials. The hysteresis loops are not symmetric about the origin. For each cycle, the tensile (compressive) modulus is defined as the slope of the linear tensile (compressive) region of the hysteresis loop, and the tensile and compressive modulus decrease with fatigue cycles, accompanied by the cyclic tensile (compressive) strain increase. The cyclic softening during compression is observed in Fig. 4, which may due to the mechanical obstruction of crack closure by matrix debris. At the same time, as the fatigue cycles increases, the cyclic thermal shocked ox/ox-CMCs also soften, and the softening rate is faster than the original ox/ox-CMCs.

From the initial loading to the stress amplitude σ_a, the matrix is cracked as well as the fiber/matrix interface is debonded. Micro-slip occurs at the fiber/matrix interface, causing the unloading/reloading stress-strain hysteresis during subsequent unloading and reloading process. The hysteresis energy density (HED) behavior mirrors the composites elastic modulus behavior, and the HED is defined by the area associated with hysteresis loops during corresponding fatigue cycles [29,31],

$$\Upsilon = \int_{\sigma_{min}}^{\sigma_{max}} [\varepsilon_N^{unloading}(\sigma) - \varepsilon_{N+1}^{reloading}(\sigma)]d\sigma \quad (1)$$

where Υ is the hysteresis energy density, $\varepsilon_N^{unloading}$ denotes the unloading strain for the N cycle, $\varepsilon_{N+1}^{reloading}$ denotes the reloading strain the $N+1$ cycle. The HED calculated by Eq. (1) using the experimental data with the cycle for the original and cyclic thermal shocked ox/ox-CMCs are illustrated in Fig. 5. The HED decreases rapidly at first and then slowly with fatigue cycles increase. The higher the applied stress level, the faster the rate at which the HED decreases. However, the HED for original ox/ox-CMCs decreases faster than the cyclic thermal shocked ox/ox-CMCs, due to that the thermal shock-induced thermomechanical damage reduces the ability of materials to withstand the cyclic load.

When the stress level is near or below the ultimate fatigue strength, the HED will decrease and then quickly stabilize to a relatively small dissipation level, the average HED value is only 12.5 kJ/m^3 for the original ox/ox-CMCs, and for the cyclic thermal shocked ox/ox-CMCs, the average HED value is only 7.0 kJ/m^3. Such a small HED value indicates that the hysteresis is small and there is little actual fatigue damage for the cyclic thermal shocked ox/ox-CMCs.

3.2. Cyclic stress-strain behavior

The Ramberg-Osgood model can be applied to describe the

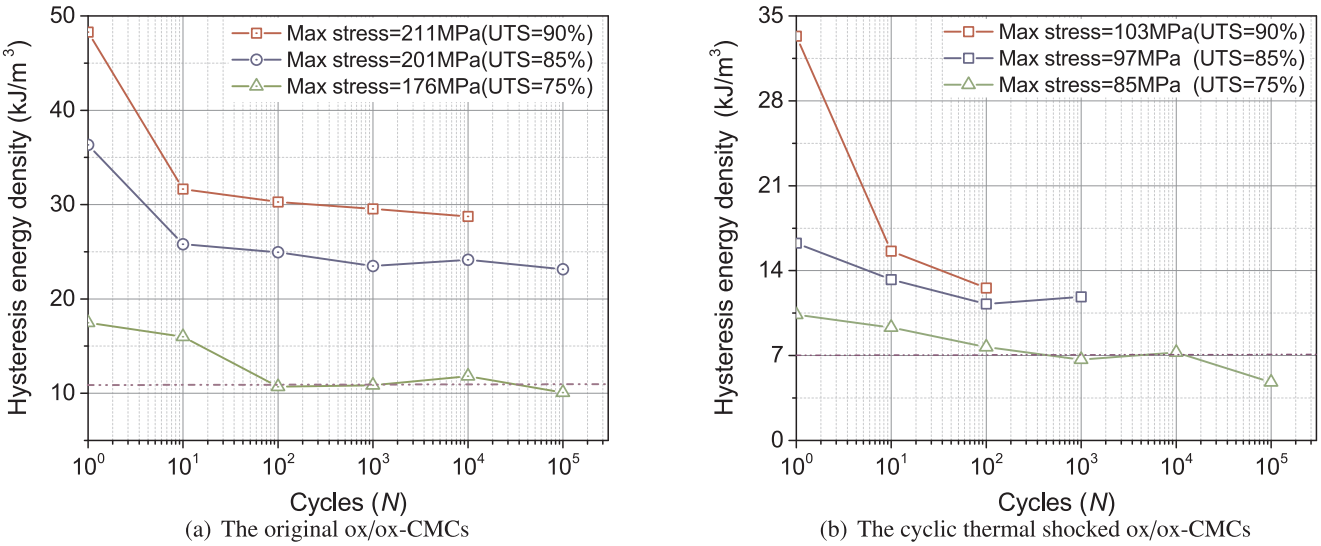

(a) The original ox/ox-CMCs (b) The cyclic thermal shocked ox/ox-CMCs

Fig. 5. Hysteretic energy density versus fatigue cycles for ox/ox-CMCs fatigue tested at three stress levels. At each stress level there is a rapid decrease in energy being absorbed by the specimen, and, after 100 cycles, the value remains constant.

monotonic tensile stress-strain behavior of ox/ox-CMCs,

$$\varepsilon = \frac{\sigma}{E} + \left(\frac{\sigma}{K}\right)^{1/n} \tag{2}$$

here K and n are the strength coefficient and the strain hardening exponent, respectively.

According to the discussion above, the cyclic stress-strain response of ox/ox-CMCs can be characterized by the cyclic stress-strain curve, and the Ramberg-Osgood model can fit the cyclic stress-strain curve as well:

$$\varepsilon_a = \frac{\sigma_a}{E} + \left(\frac{\sigma_a}{K'}\right)^{\frac{1}{n'}} \tag{3}$$

where K' is the cyclic strength coefficient, n' is the cyclic strain hardening exponent. The experimental model parameters for the original and cyclic thermal shocked ox/ox-CMCs are summarized in Table 1.

The stress-strain curves of both materials under uniaxial monotonic and cyclic loading are obtained according to Eqs. (2) and (3), which are illustrated in Fig. 6.

As for the cyclic stress-strain curves, the strain amplitude for each loading path is computed from the stable cycle of each specimen. The symbols and the lines represent experimental data and the predicted results of the monotonic and cyclic Ramberg-Osgood model for the original and cyclic thermal shocked ox/ox-CMCs, respectively. The fracture strain of the cyclic thermal shocked ox/ox-CMCs is significantly reduced compared with the original ones. Cyclic thermal shock-induced thermomechanical damage results in lower fracture toughness for the cyclic thermal shocked ox/ox-CMCs. Both the cyclic strength coefficient K' and the cyclic strain hardening exponent n' increase for the cyclic thermal shocked ox/ox-CMCs. Furthermore, for the same strain level, the cyclic stress of the cyclic thermal shocked ox/ox-CMCs is much lower than that of the original ox/ox-CMCs, indicating that the cyclic thermal shock causes the effective load capacity of the material to decrease, as well as reduce the material resistant to cyclic deformation.

3.3. Evolution of cumulative strain with fatigue cycles

The evolutions of the accumulated strain with fatigue cycles of the original and cyclic thermal shocked ox/ox-CMCs at different stress levels are investigated, as shown in Fig. 7. Strain ratcheting and accumulation are not seen at first in all fatigue tests of both ox/ox-CMCs, but only as cycle numbers increases, the phenomena can be observed. The inelastic deformation in ox/ox-CMCs is mainly caused by the initiation and propagation of matrix cracks. Generally, lower strain accumulation with cycles implies that less damage occurs, which is mostly limited to some additional matrix cracking. However, in this case, low accumulated strains are more likely caused by early bundle failures and finally lead to specimen failure.

It can be seen from Fig. 7(a) that, for the original ox/ox-CMCs, when the test stress level is over the ultimate fatigue strength (75% UTS), there is no strain ratchet effect and the strain accumulation can be neglected in the early stage of the fatigue tests. After about 200 cycles, the strain ratchet develops rapidly and the compression region accumulates significant permanent strain. However, as shown in Fig. 7(b), strain accumulation for the cyclic thermal shocked ox/ox-CMCs is faster, especially at a higher stress level (90% UTS). It indicates that the cyclic softening process is related to the cyclic thermal shocks experienced. The cyclic thermal shock causes the loss of matrix porosity, which in turns changes the material responds to cyclic loading, while the macroscopic stiffness of original ox/ox-CMCs is higher to resistance to deformation, leading the cycle softening rate slower.

3.4. Evolution of elastic modulus with fatigue cycles

The reduction in stiffness during fatigue cycling reflects fatigue damage development. The changes in the elastic modulus with the fatigue cycles of the original and cyclic thermal shocked ox/ox-CMCs are measured respectively to reflect the damage evolution during the fatigue cycles. Due to the dispersion of the composite materials, the initial elastic portion of the first cyclic loading section does not have sufficient data, so the unloading modulus of the first cycle is used as a reference, that is, the change of elastic modulus is presented in the form of the normalized modulus related to the unloading modulus in the first cycle ($\widetilde{E}/E_{\text{unloading}}$).

Fig. 8 shows the normalized elastic modulus as a function of fatigue cycles of the original and cyclic thermal shocked ox/ox-CMCs at different stress levels. Since the dispersion of the materials is too large, each curve is divided by its own modulus for normalization, and typical curves are selected for analysis.

Whether the test specimens fail or not, the elastic modulus decreases continuously with fatigue cycles. The reduction in the elastic modulus consists of two stages: the elastic modulus decreases continuously with fatigue cycles in the first few cycles, and then a rapid decrease in elastic modulus is observed before failure, caused by the matrix crack coalescence and pull-out or fracture of fibers.

Obviously, for the failed specimens, the reduction of the normalized modulus for cyclic thermal shocked ox/ox-CMCs is significantly faster, as shown in Fig. 8(b), suggesting that the cyclic thermal shocks accelerate the material elastic modulus degradation. Although some specimens tested reached the fatigue run-out of 2×10^5 cycles, the normalized modulus still decreases with cycles. When the fatigue limit is reached, the elastic modulus loss of the cyclic thermal shocked ox/ox-CMCs is 12%, which is consistent with the original ox/ox-CMCs.

3.5. Fatigue failure mechanisms

Generally, the damage in composites includes fiber debonding, matrix cracking and fiber sliding, which also can be observed in the fatigue tests. The fracture surfaces of the original and thermal shocked ox/ox-CMCs in tension-compression fatigue tests at the same stress level (90% UTS) are shown in Fig. 9(a)-(b). The fracture surface of the original ox/ox-CMCs is relatively flat. Conversely, the thermal shocked ox/ox-CMCs produces fiber breakage and have significantly long damage zones (ca. 20 mm), which may be related to cyclic thermal shock-induced thermomechanical damage associated.

To gain a deep understanding of the mechanism of a sudden decrease in fatigue life during cyclic loading, the fracture surfaces of the fatigue specimens are observed by SEM. The critical feature of the fracture surface has a large amount of compression crimped fiber fracture caused by micro-buckling of the fibers.

Since the porous matrix in the ox/ox-CMCs is very fragile, the fiber bears most of the load during the tensile loading process. Therefore, the buckling and fracture of the 0° fiber bundles result in a decrease in effective load capacity of the materials. The damage and failure mechanism of the original ox/ox-CMCs in tensile-compression fatigue tests is a large number of fiber breakages caused by micro-buckling of the fiber under cyclic compressive loading, as shown in Fig. 9(c). In the 0°/90° cross-lay, matrix cracks form between adjacent fibers in the 0° layer, then grow subcritically to form a shear zone gradually, causes the fiber to bend and buckle. Fig. 9(d) reveals the fiber bending of the composites under cyclic tensile-compression loading. The bending stress

Table 1
Model parameters of the original and cyclic thermal shocked ox/ox-CMCs.

Material	Monotonic		Cyclic	
Behavior	K (MPa)	n	K' (MPa)	n'
Original	41740	0.842	4274	0.49
Thermal shocked	11370	0.712	8606	0.67

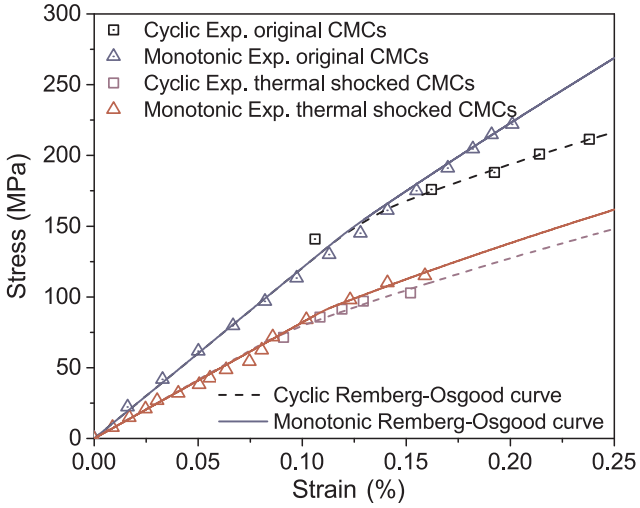

Fig. 6. The stress-strain curves of both materials under uniaxial monotonic and cyclic loading.

generated by in-phase buckling in the fiber results in the formation of a kink zone and subsequent brittle fiber fracture.

4. Theoretical fatigue damage model

The fatigue damage is a progressive and irreversible process and its accumulation brings the materials to failure. Generally, the residual strength, residual stiffness and life can be used to predict the fatigue damage of ox/ox-CMCs. However, in actual application, it is necessary to determine the fatigue damage of structures nondestructively after servicing a period [32]. Therefore, the residual stiffness is an excellent choice to predict the failure of ox/ox-CMCs, which is easy to measure and interpret, as the residual strength and life may involve the destruction of the test specimens.

To quantify the fatigue damage based on the recorded stress-strain hysteresis loops under cyclic loading, the material damage under uniaxial loading can be defined by the variation of elastic modulus, as

$$D = 1 - \frac{E}{E_0} \tag{4}$$

where E denotes the actual elastic modulus of the damage materials, and E_0 is the initial elastic modulus. Hence, the fatigue damage evolution of materials is characterized by the decrease of elastic modulus.

Fig. 10 illustrates the damage evolution in the tension-compression case with different stress levels, in which the total damage D is plotted with loading cycles, and the evolution consists of two stages: The damage occurs at the initial stage and increases continuously with loading cycles. Then, due to the saturation of the matrix crack density, the fracture and pull-out of the fiber, the fracture strain of the materials reaches the critical value ε^{cr}, and the damage develops rapidly before rupture. The critical damage value D^{cr} at the rupture of specimen is observed in Fig. 10(a).

The fatigue loading can be regarded as two parts: (i) the monotonic loading (in the first half loading cycle); and (ii) the cyclic loading. Therefore, based on the damage model of the cyclic thermal shocked ox/ox-CMCs in the monotonic loading, the total thermomechanical damage can be decoupled into two parts: the elastic damage D_e driven by elastic strain energy density, and fatigue damage D_f driven by plastic strain energy under cyclic loading, that is

$$\dot{D} = \dot{D}_e + \dot{D}_f \tag{5}$$

Hypothesis the cyclic thermal shock-induced thermomechanical damage is elastic damage, and the damage gradually grows to saturation with thermal shock cycles. A quantitative description of the thermomechanical damage model is discussed in [7]. The fatigue damage D_f can grow, once $\varepsilon < \varepsilon^{cr}$. Of particular note is that the plastic strain energy is the only driving force leading to the accumulation of fatigue damage of ox/ox-CMCs. The fatigue damage D_f can be represented by the total thermomechanical damage, D,

$$D_f = D - D_e \tag{6}$$

where D_e is the sum of the mechanical elastic damage in the first half loading cycle D_e^1 and the pre-damage D_{shock}, that is $D_e = D_e^1 + D_{shock}$ [33]. Neglected the mechanical elastic damage in the first half loading cycle for the sake of simplicity, more general description of the ox/ox-CMCs mechanical damage will be discussed in a separate paper. Here only the cyclic thermal shock-induced thermomechanical damage in the composites is considered. Fig. 10 (b) illustrates the variation the fatigue damage vs. the loading cycles according to Eq. (6).

4.1. Quantitative description of thermal shocks-induced thermomechanical damage

According to the thermodynamics of continuum damage mechanic, the thermodynamical forces associated with the dissipative mechanisms

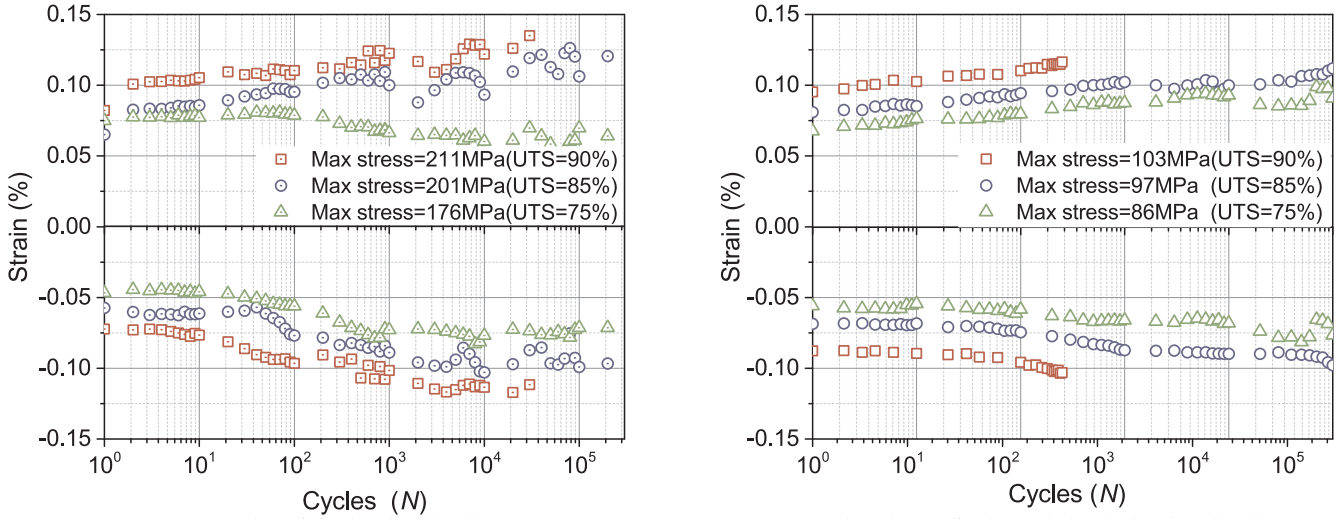

(a) The original ox/ox-CMCs (b) The cyclic thermal shocked ox/ox-CMCs

Fig. 7. The maximum and minimum strains vs. cycles.

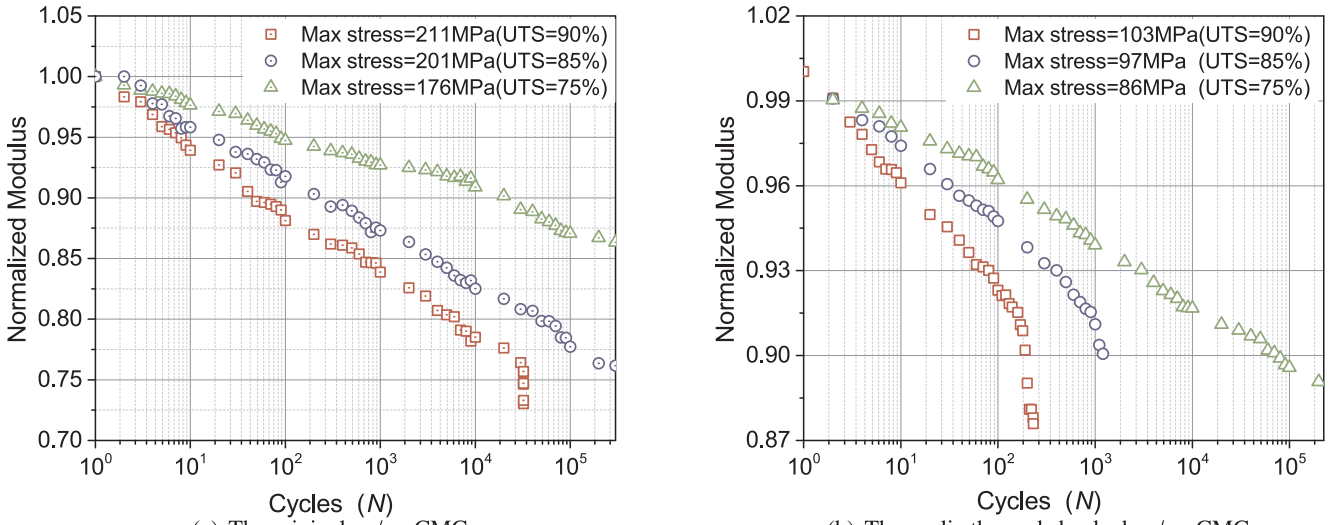

(a) The original ox/ox-CMCs (b) The cyclic thermal shocked ox/ox-CMCs

Fig. 8. Normalized tensile modulus vs. fatigue cycles for ox/ox-CMCs tested under three stress levels.

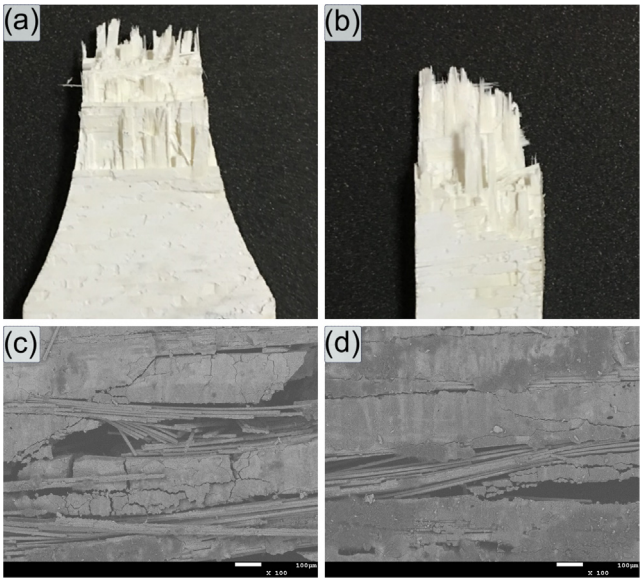

Fig. 9. (a) Fracture surfaces of the original ox/ox-CMCs specimens at stress level of 90% UTS, (b) fracture surfaces of the thermal shocked ox/ox-CMCs specimens at stress level of 90% UTS, (c) fiber breakage, (d) fiber bundle bending.

can be derived from the energy release rates [10],

$$Y = \rho\frac{\partial\Phi}{\partial D}. \tag{7}$$

above ρ is density, and Φ is the dissipation potential, which consists of strain energy density $\varphi = \varphi(\varepsilon_{ij}, \varepsilon_{ij}^{p}, D)$ and the dissipation term $\pi(\delta, p)$ [34],

$$\Phi = \varphi(\varepsilon_{ij}, \varepsilon_{ij}^{p}, D) + \pi(\delta, p) \tag{8}$$

where ε_{ij}^{p} is the plastic strain, p is the thermodynamic force-flux parameter associated to plastic hardening, and δ is the thermodynamic force-flux parameter associated to damage hardening [34]. Due to that the ox/ox CMCs didn't show the plastic hardening and damage hardening phenomenon during the fatigue loading, p and δ can be ignored in this work. Therefore, the dissipation potential can be rewritten as,

$$\rho\Phi = \frac{1}{2\rho}\widetilde{E}_{ijkl}\varepsilon_{ij}^{e}\varepsilon_{kl}^{e}(1-D), \tag{9}$$

Substituting Eq. (9) into Eq. (7), then

$$Y = \frac{1}{2}\widetilde{E}_{ijkl}\varepsilon_{ij}^{e}\varepsilon_{kl}^{e} = \frac{\widetilde{\sigma}_{eq}^{2}}{2E_0}f(\eta), \tag{10}$$

where $\widetilde{\sigma}_{eq}$ is the effective stress, and $f(\eta)$ is the function of the stress triaxiality η. For isotropic materials, $f(\eta)$ is defined as [10],

$$f(\eta) = \frac{2}{3}(1+\nu) + (1-2\nu)\eta^{2}. \tag{11}$$

The second principle of thermodynamics is contented, which is written as the Clausius-Duhem inequality:

$$\sigma_{ij}\dot{\varepsilon}_{ij} + Y\dot{D} \geqslant 0. \tag{12}$$

as the dissipation is positive, the damage evolution laws should meet the following equation: $\dot{D} \geqslant 0$.

Obviously, with the shock cycles N increase, the strain energy of the materials will decreases as the cyclic thermal shock cause the damage D in the materials. In other words, the damage increment ΔD from cycle to cycle leads to the strain energy dissipation, as the damage is the only energy consumer. In order to illustrate the relationship between the damage and the energy dissipation, the energy dissipation can be defined as,

$$\Pi_{N} = \sum_{k=1}^{N}(Y_{k-1} - Y_{k}). \tag{13}$$

where Y_k is the strain energy in the materials after kth thermal shock. Then the total energy dissipation for a given shock temperature can be derived as [8],

$$\Pi_{N} = Y_0(2-D)D. \tag{14}$$

where Y_0 is the initial strain energy. Eq. (14) illustrates the relationship between the total energy dissipation and the damage.

4.2. Progressive damage model

From the perspective of the microscopic failure mechanism, the cyclic plastic strain is related to slips and reverses slips at the fiber/matrix interface. The fatigue damage of each cycle can be characterized by the plastic strain energy of each cycle.

In uniaxial loading case, the plastic strain energy density ΔW^{p} can be expressed as

$$\Delta W^{p} = \oint \sigma d\varepsilon^{p} \tag{15}$$

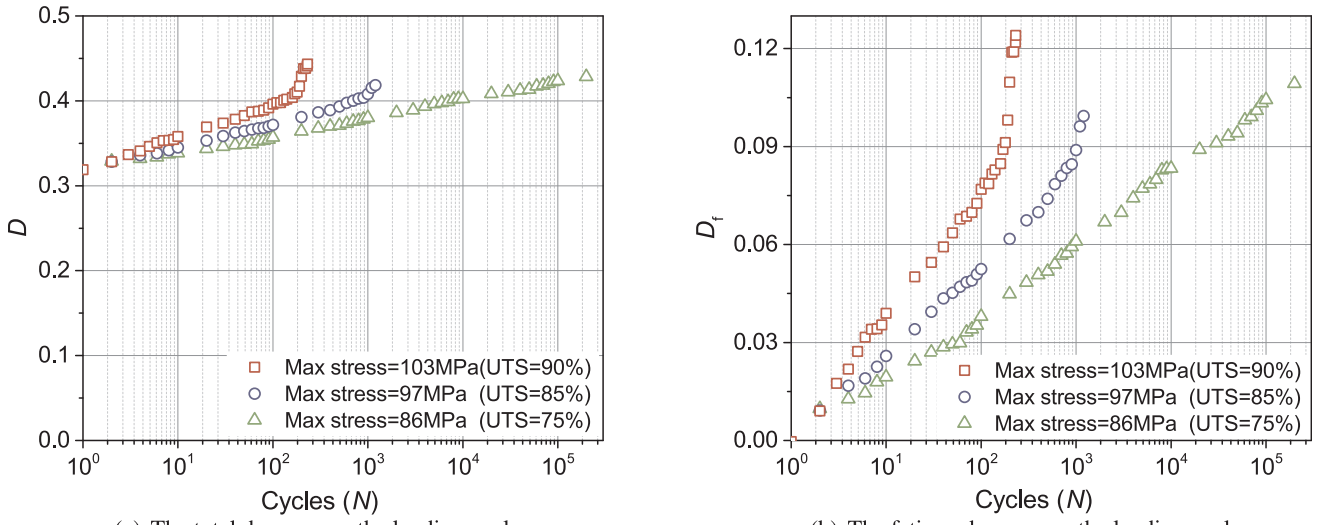

(a) The total damage vs. the loading cycles (b) The fatigue damage vs. the loading cycles

Fig. 10. Damage evolution curves identified in the uniaxial fatigue tests with different stress amplitude for the thermal shocked ox/ox-CMCs. (a) The total damage vs. number of cycles, (b) the fatigue damage vs. number of cycles based on Eq. (6).

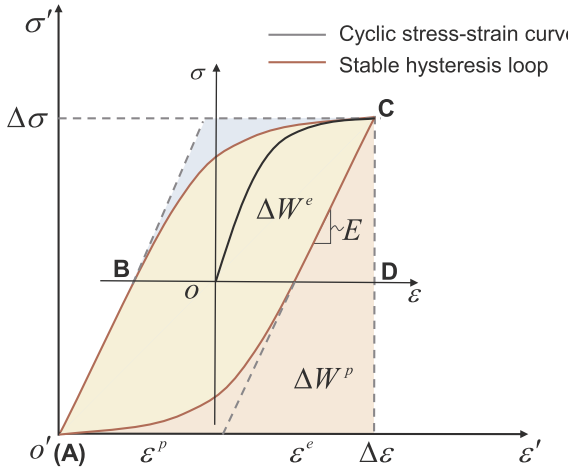

Fig. 11. The schematic diagram of the plastic strain energy density.

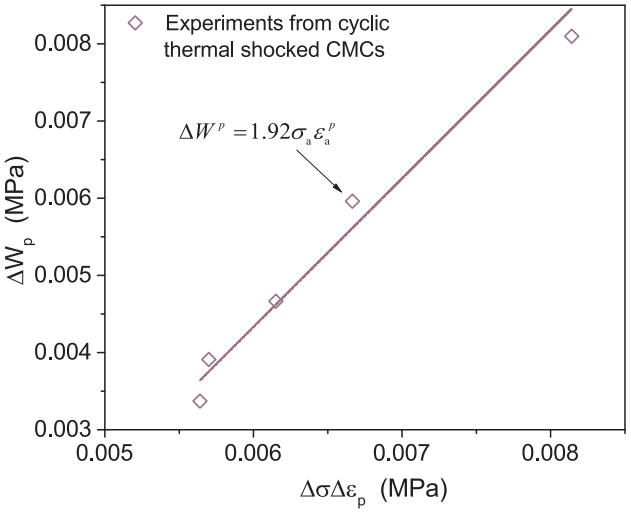

Fig. 12. Correlation between the plastic strain energy on the critical plane within one cycle and the product of the effective stress and strain ranges.

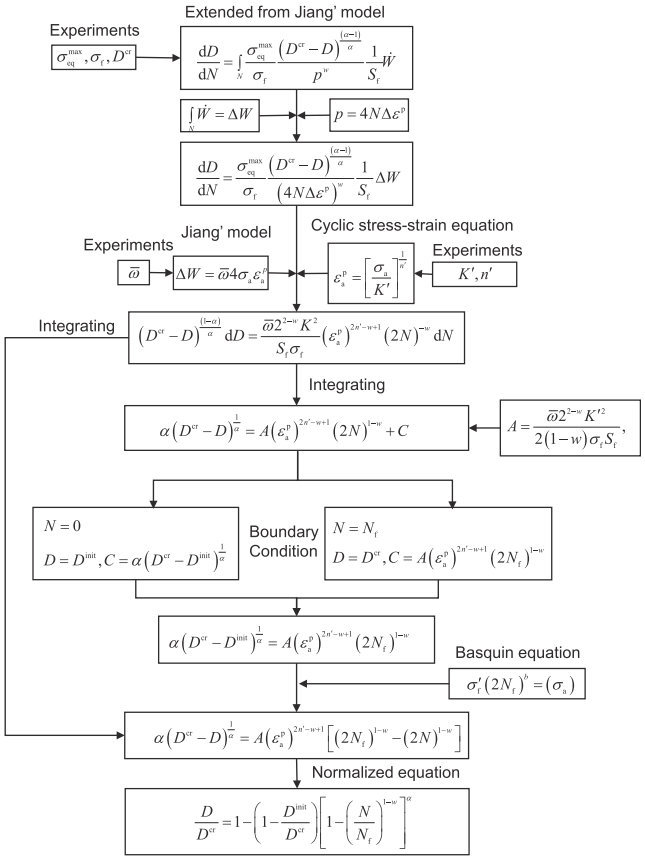

Fig. 13. Flowchart of the proposed model.

To calculate the plastic strain energy density ΔW^p , firstly, the stress-strain relation equation is needed to describe the shape of the hysteresis stress-strain loop. Then the plastic strain energy density is calculated by numerical integration of the stable hysteresis loop, as illustrated in Fig. 11.

Jiang found that there is a linear relationship between the plastic strain energy density ΔW^p and the product of stress amplitude and plastic strain amplitude $\sigma_a\varepsilon_a^p$. For uniaxial cyclic tension-compression cases [35],

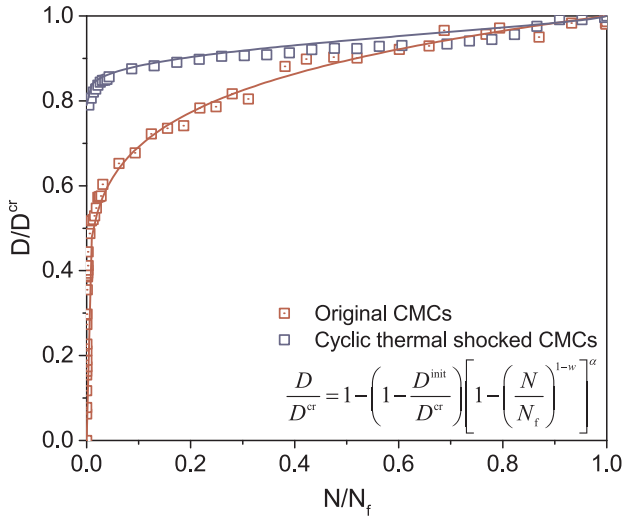

Fig. 14. Tensile-compression damage evolution curve of ox/ox-CMCs.

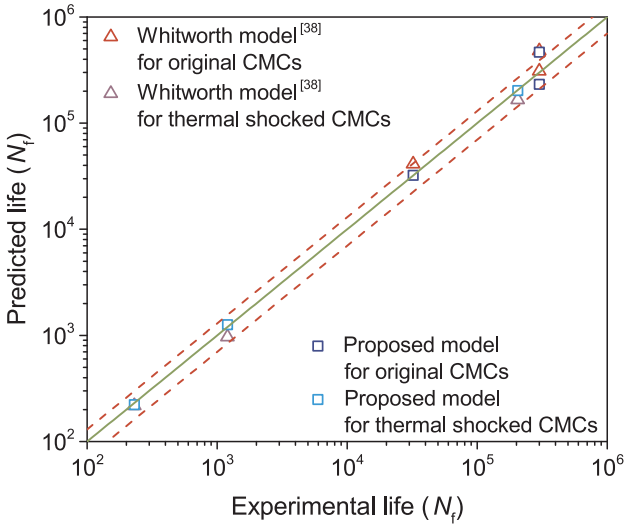

Fig. 15. Comparison of fatigue life prediction between the original and cyclic thermal shocked ox/ox-CMCs.

$$\Delta W^{p}=\bar{\omega}\Delta\sigma\Delta\varepsilon^{p} \tag{16}$$

where $\bar{\omega}$ is a factor, indicating the effect of different strain energy components. Fig. 12 show the correlation between the plastic strain energy on the critical plane within one cycle and the product of the effective stress and strain ranges for cyclic thermal shocked ox/ox-CMCs.

To describe the damage evolution under fatigue loading conditions, most researchers use the power law to establish the fatigue models, which are different in quantifying material properties and the damage evolution. In the present study, a new fatigue damage model is extended from Jiang's model to describe the fatigue damage evolution of ox/ox-CMCs in the low cycle fatigue, with the driving force being plastic strain energy ΔW^{p} [35,36]. The fatigue damage growth rate $\dot{D}_f$ is defined as [37]

$$\dot{D}_f=\frac{\sigma_{eq}^{max}}{\sigma_f}\frac{(D^{cr}-D)^{\frac{(\alpha-1)}{\alpha}}}{p^{w}}\frac{1}{S_f}\dot{W} \tag{17}$$

where σ_{eq}^{max} is the maximum equivalent Mises stress and the mean stress effect on the fatigue damage development. σ_f is the fracture stress determined in the monotonic tensile experiment. The term $(D^{cr}-D)^{\frac{(\alpha-1)}{\alpha}}$ considers the different form of damage evolution curves. Additionally, p^{w} takes into account the influence of the accumulated plastic deformation in the fatigue damage process. Here, the parameters α, w, S_f are material parameters.

The following assumption can be used to simplify the derivation: (i) During one cycle, the change of the damage D is small so that D is supposed to be constant in one cycle; (ii) The variation of accumulated plastic strain in one cycle is negligible. Based on the above assumption, the damage over the whole cycles can be viewed as the accumulation of D of each cycle. Then, the fatigue damage evolution is re-written as:

$$\frac{dD}{dN}=\int_N\frac{\sigma_{eq}^{max}}{\sigma_f}\frac{(D^{cr}-D)^{\frac{(\alpha-1)}{\alpha}}}{p^{w}}\frac{1}{S_f}\dot{W} \tag{18}$$

the accumulated plastic strain energy in one cycle is written with $\int_N\dot{W}=\Delta W$, and $p=4N\Delta\varepsilon^{p}$. Eq. (18) can be rewritten as

$$\frac{dD}{dN}=\frac{\sigma_{eq}^{max}}{\sigma_f}\frac{(D^{cr}-D)^{\frac{(\alpha-1)}{\alpha}}}{(4N\Delta\varepsilon^{p})^{w}}\frac{1}{S_f}\Delta W \tag{19}$$

a linear equation $\Delta W=\bar{\omega}4\sigma_a\varepsilon_a^{p}$ is used to approximate ΔW. Cyclic plastic deformation plays an important role in low cycle fatigue life analysis of materials. An appropriate constitutive method is needed to calculate the estimated stress and strain of fatigue damage parameters. The cyclic stress-strain equation can be used to determine the relationship between the stress amplitude σ_a and the plastic strain amplitude ε_a^{p}:

$$\varepsilon_a^{p}=\left[\frac{\sigma_a}{K'}\right]^{\frac{1}{n'}}. \tag{20}$$

Substituting the Eq. (20) into Eq. (19), one obtains

$$(D^{cr}-D)^{\frac{(1-\alpha)}{\alpha}}dD=\frac{\bar{\omega}2^{2-w}K'^{2}}{S_f\sigma_f}(\varepsilon_a^{p})^{2n'-w+1}(2N)^{-w}dN \tag{21}$$

Integrating the Eq. (21), then

$$\alpha(D^{cr}-D)^{\frac{1}{\alpha}}=A(\varepsilon_a^{p})^{2n'-w+1}(2N)^{1-w}+C \tag{22}$$

where the term A is

$$A=\frac{\bar{\omega}2^{2-w}K'^{2}}{2(1-w)\sigma_f S_f},$$

and C is a constant depending on boundary condition. For $N=0$, $D=D^{init}$, $C=\alpha(D^{cr}-D^{init})^{\frac{1}{\alpha}}$, D^{init} refers to the initial (pre-) damage contained in the materials. For the cyclic thermal shocked ox/ox-CMCs, D^{init} refers to the thermomechanical damage caused by cyclic thermal shocks. In addition, when the material fails after $N=N_f$ cycles, $D=D^{cr}$, so that $C=A(\varepsilon_a^{p})^{2n'-w+1}(2N_f)^{1-w}$. Then it can be deduced that,

$$\alpha(D^{cr}-D^{init})^{\frac{1}{\alpha}}=A(\varepsilon_a^{p})^{2n'-w+1}(2N_f)^{1-w}. \tag{23}$$

Then, defining the term $B=\frac{\alpha(D^{cr}-D^{init})^{\frac{1}{\alpha}}}{A}$, and substituting B into Eq. (23), the following is obtained,

$$B(2N_f)^{w-1}=(\varepsilon_a^{p})^{2n'-w+1} \tag{24}$$

Since the fatigue experiments are under stress control, a power law relation between the stress amplitude σ_a and the fatigue life N_f is given corresponding the Basquin equation,

$$\sigma'_f(2N_f)^{b}=(\sigma_a) \tag{25}$$

where b notes fatigue strength exponent, and σ_f' notes fatigue strength coefficient. Integrating Eq. (21) from N to N_f and D to D^{cr}, the damage can be expressed as,

$$\alpha(D^{cr}-D)^{\frac{1}{\alpha}}=A(\varepsilon_a^{p})^{2n'-w+1}[(2N_f)^{1-w}-(2N)^{1-w}] \tag{26}$$

Combining Eq. (23) with Eq. (26), the relation between damage and cycle numbers under uniaxial loading can be found as:

$$\frac{D}{D^{cr}} = 1 - \left(1 - \frac{D^{init}}{D^{cr}}\right)\left[1 - \left(\frac{N}{N_f}\right)^{1-w}\right]^{\alpha} \quad (27)$$

Fig. 13 illustrates the flowchart of the proposed model, and the parameters taken from experiment are stated in the flowchart. Fig. 14 shows the damage evolution of the original and cyclic thermal shocked ox/ox-CMCs at the stress level of 90% UTS. Both render the same form of fatigue damage evolution: in the tension-compression cyclic loading tests, damage occurs during the first few cycles, and then grows gradually to a stable phase. The damage evolution of the cyclic thermal shocked ox/ox-CMCs is characterized by two stages:

- In the primary phase, the damage begins as soon as the specimen subjected to cyclic loading. Since the material consists of a porous matrix, the matrix micro-cracks will quickly deflect to the fiber/matrix interface, resulting in a rapid decrease in the elastic modulus.
- Material fatigue damage is related to fiber/matrix interface delamination and friction. As fibers dominate the stretching process, higher forces are required for fiber breakage/pull-out. The damage development tends to be stable and the growth rate of damage is low (the curve of red circle in Fig. 14). When the accumulated plastic strain exceeds the critical fracture strain, the material finally failed.

4.3. The predict life of the progressive damage model

As the model parameters of the original and the cyclic thermal shocked ox/ox-CMCs at different stress levels are obtained through experimental data, the obtained models are used for fatigue life prediction, as shown in Fig. 15. The solid line indicates that the predicted results are identical with experimental results, and the two dotted lines are the boundaries of 30% errors. The life results predicted by the two models are in good agreement with the experimental results. For the thermal shocked CMCs, the difference between the Whitworth model [38] and the experimental results is up to 28%, and the progressive damage growth model is up to 5%. On the other hand, for the original CMCs, both models show around 40% difference with the experiments at 75% UTS. Therefore, the progressive damage growth model has a good predictive effect and can be used for the life prediction of the cyclic thermal shocked ox/ox-CMCs.

5. Conclusions

In this paper, the fatigue damage evolution, cyclic stress-strain response, and fatigue life prediction of the original and thermal shocked ox/ox-CMCs under uniaxial tensile-compression cyclic loading are studied. The main conclusions are:

- The ultimate fatigue strength of the original ox/ox-CMCs in the tensile-compression fatigue is up to 85% of the average UTS, and the fatigue failure mechanism is fiber buckling under compression load. The fatigue limit strength of the cyclic thermal shocked ox/ox-CMCs in the tension-compression fatigue is only 75% UTS. The failure mechanism is that a large number of matrix micro-cracks and local delamination occur in the matrix due to cyclic thermal shocks, which further reduces the fatigue limit of the ox/ox-CMCs.
- The cyclic stress-strain curve of ox/ox-CMCs is different from the monotonic stress-strain curve. Both the original and cyclic thermal shocked ox/ox-CMCs undergo cyclic softening in the whole loading history. Even at a lower stress level which the materials can reach the fatigue limit, its elastic modulus still drops, which is further confirmed by the cyclic hysteresis energy density theory.
- To describe the evolution of fatigue damage in the cyclic thermal shocked ox/ox-CMCs, a nonlinear fatigue damage model based on Jiang's model and continuum damage mechanics is proposed. The total damage consists of the thermal stress-related damage from thermal shocks and the fatigue damage from applied mechanical loads. The plastic strain energy density is used as the damage driving force in fatigue damage. The fatigue damage evolution law is combined with the Ramberg-Osgood cyclic plastic model to predict the cyclic deformation and accumulation process of the damage.

Declaration of Competing Interest

The authors declare that they have no known competing financial interests or personal relationships that could have appeared to influence the work reported in this paper.

Acknowledgement

The present work is supported by the Strategic Priority Research Program of Chinese Academy of Sciences (Grant No. XDA17030100), the National Natural Science Foundation of China (Grant No. 11572169 and 51775294).

References

[1] Sedrakian A, Zineb TB, Billoet JL. Contribution of industrial composite parts to fatigue behaviour simulation. Int J Fatigue 2002;24(2):307–18.
[2] Brighenti R. Numerical modelling of the fatigue behavior of fibre-reinforced composites. Compos Part B: Eng 2004;35(3):197–210.
[3] Wilkinson MP, Ruggles-Wrenn MB. Fatigue of a 2D unitized polymer/ceramic matrix composite at elevated temperature. Polym Testing 2016;54:203–13.
[4] Yang Z, Liu H. Effects of thermal aging on the cyclic thermal shock behavior of oxide/oxide ceramic matrix composites. Mater Sci Eng A 2020;769:138494. https://doi.org/10.1016/j.msea.2019.138494.
[5] Wang H, Singh RN, Lowden RA. Thermal shock behavior of two-dimensional woven fiber-reinforced ceramic composites. J Am Ceram Soc 1996;79(7):1783–92.
[6] Kastritseas C, Smith PA, Yeomans JA. Thermal shock fracture in unidirectional fibre-reinforced ceramic-matrix composites. Compos Sci Technol 2005;65(11–12):1880–90.
[7] Yang Z, Yuan H, Liu H. Evolution and characterization of cyclic thermal shock-induced thermomechanical damage in oxide/oxide ceramics matrix composites. Int J Fatigue 2019;120:150–61.
[8] Yang Z, Yuan H, Markert B. Representation of micro-structural evolution and thermo-mechanical damage in thermal shocked oxide/oxide ceramic matrix composites. Int J Fatigue 2019;126:122–9.
[9] Yang Z, Liu H, Yuan H. Micro-porosity as damage indicator for characterizing cyclic thermal shock-induced anisotropic damage in oxide/oxide ceramic matrix composites. Eng Fract Mech 2019;220:106669. https://doi.org/10.1016/j.engfracmech.2019.106669. UNSP 106669.
[10] Lemaitre J, Desmorat R. Engineering damage mechanics: ductile, creep, fatigue and brittle failures. Berlin Heidelberg: Springer-Verlag; 2005.
[11] Heathcote JA, Gong X-Y, Yang JY, Ramamurty U, Zok FW. In-plane mechanical properties of an all-oxide ceramic composite. J Am Ceram Soc 2004;82(10):2721–30.
[12] Ruggles-Wrenn MB, Lanser RL. Tension-compression fatigue of an oxide/oxide ceramic composite at elevated temperature. Mater Sci Eng A-Struct Mater Properties Microstruct Process 2016;659:270–7.
[13] Chen Y, Zhao Y, He C, Ai S, Lei H, Tang L, et al. Yield and failure theory for unidirectional polymer-matrix composites. Compos Part B: Eng 2019;164:612–9.
[14] Degrieck J, Van Paepegem W. Fatigue damage modeling of fibre-reinforced composite materials: Review. Appl Mech Rev 2001;54(4):279.
[15] Mohammadi B, Fazlali B, Salimi-Majd D. Development of a continuum damage model for fatigue life prediction of laminated composites. Compos Part A: Appl Sci Manuf 2017;93:163–76.
[16] Wicaksono S, Chai GB. Life prediction of woven CFRP structure subject to static and fatigue loading. Compos Struct 2015;119:185–94.
[17] Chaboche JL, Maire JF. New progress in micromechanics-based CDM models and their application to CMCs. Compos Sci Technol 2001;61(15):2239–46.
[18] Chaboche JL, Kanoute P, Azzouz F. Cyclic inelastic constitutive equations and their impact on the fatigue life predictions. Int J Plast 2012;35:44–66.
[19] Min JB, Xue D, Shi Y. Micromechanics modeling for fatigue damage analysis designed for fabric reinforced ceramic matrix composites. Compos Struct 2014;111:213–23.
[20] Sabelkin V, Mall S, Cook TS, Fish J. Fatigue and creep behaviors of a SiC/SiC composite under combustion and laboratory environments. J Compos Mater 2015;50(16):2145–53.
[21] Benkabouche S, Guechichi H, Amrouche A, Benkhettab M. A modified nonlinear fatigue damage accumulation model under multiaxial variable amplitude loading. Int J Mech Sci 2015;100:180–94.
[22] Li L. Modeling thermomechanical fatigue hysteresis loops of long-fiber-reinforced ceramic-matrix composites under out-of-phase cyclic loading condition. Int J Fatigue 2017;105:34–42.
[23] Rafiee R, Elasmi F. Theoretical modeling of fatigue phenomenon in composite pipes. Compos Struct 2017;161:256–63.
[24] Rafiee R, Torabi MA. Stochastic prediction of burst pressure in composite pressure

vessels. Compos Struct 2018;185:573–83.
[25] Rafiee R. Stochastic fatigue analysis of glass fiber reinforced polymer pipes. Compos Struct 2017;167:96–102.
[26] Rafiee R, Sharifi P. Stochastic failure analysis of composite pipes subjected to random excitation. Constr Build Mater 2019;224:950–61.
[27] Yang Z, Yang J. Investigation of long-term thermal aging-induced damage in oxide/oxide ceramic matrix composites. J Eur Ceram Soc. doi: 10.1016/j.jeurceramsoc.2019.10.052.
[28] Opila EJ, Myers DL. Alumina volatility in water vapor at elevated temperatures. J Am Ceram Soc 2008;87(9):1701–5.
[29] Zawada LP, Hay RS, Lee SS, Staehler J. Characterization and high-temperature mechanical behavior of an oxide/oxide composite. J Am Ceram Soc 2003;86(6):981–90.
[30] Ruggles-Wrenn MB, Hetrick G, Baek SS. Effects of frequency and environment on fatigue behavior of an oxide–oxide ceramic composite at 1200 °C. Int J Fatigue 2008;30(3):502–16.
[31] Van Paepegem W, Degrieck J, De Baets P. Finite element approach for modelling fatigue damage in fibre-reinforced composite materials. Compos Part B: Eng 2001;32(7):575–88.
[32] Quaresimin M, Carraro PA, Mikkelsen LP, Lucato N, Vivian L, Brøndsted P, et al. Damage evolution under cyclic multiaxial stress state: a comparative analysis between glass/epoxy laminates and tubes. Compos Part B: Eng 2014;61:282–90.
[33] Yang Z, Liu H. A continuum damage mechanics model for 2-D woven oxide/oxide ceramic matrix composites under cyclic thermal shocks. Ceram Int 2019. https://doi.org/10.1016/j.ceramint.2019.11.060.
[34] Barbero E. Finite element of composite materials. CRC Press; 2008.
[35] Jiang Y, Zhang J. Benchmark experiments and characteristic cyclic plasticity deformation. Int J Plast 2008;24(9):1481–515.
[36] Jiang Y, Ott W, Baum C, Vormwald M, Nowack H. Fatigue life predictions by integrating EVICD fatigue damage model and an advanced cyclic plasticity theory. Int J Plast 2009;25(5):780–801.
[37] Ma S, Yuan H. A continuum damage model for multi-axial low cycle fatigue of porous sintered metals based on the critical plane concept. Mech Mater 2017;104:13–25.
[38] Whitworth HA. A stiffness degradation model for composite laminates under fatigue loading. Compos Struct 1997;40(2):95–101.